Materials Science and Engineering A 381 (2004) 381–385

www.elsevier.com/locate/msea

Creep behavior and threshold stress of an extruded Al–6Mg–2Sc–1Zr alloy

S.P. Deshmukh [a], R.S. Mishra [a,*], K.L. Kendig [b]

[a] *Department of Metallurgical Engineering, University of Missouri-Rolla, Rolla, MO 65409, USA*
[b] *Air Force Research Laboratory, Materials and Manufacturing Directorate, Wright Patterson AFB, OH 45433, USA*

Received 12 April 2004; received in revised form 7 May 2004

Abstract

Creep experiments were performed on extruded Al–6Mg–2Sc–1Zr (wt.%) alloy in a temperature range of 423–533 K. A threshold type creep behavior was measured and explained by observed dislocation-particle interactions. The experimental threshold stress values at various temperatures were compared with existing theoretical models. None of the available models could account for the decrease in threshold creep strength with increasing temperature.

Keywords: Aluminum alloy; Creep test; Threshold stress

1. Introduction

Commercial aluminum alloys for high performance applications can be used up to 423–443 K range. Above this, the alloy strength degrades quickly with time in service due to rapid coarsening of fine strengthening precipitates. To increase the strength at high temperature, fine thermally stable precipitates are required which can restrict the motion of dislocations. Significant past research have been conducted to develop new aluminum alloy for high temperature applications.

Scandium containing aluminum alloys have received considerable attention in the last few years because of the remarkable strengthening effect of Sc additions [1–3]. Aluminum forms a thermodynamically stable, coherent Al_3Sc precipitate with a scandium additions. Al_3Sc has the $L1_2$ type ordered face centered cubic structure with a lattice parameter of 0.410 nm, which is similar to aluminum. The similarity of lattice parameter and structure of Al_3Sc to those of the aluminum matrix leads to a high resistance to precipitate coarsening in these alloys [3]. Most of the earlier works on Al–Sc alloys focused on hypoeutectic compositions, i.e. Sc contents below 0.6 wt.% [3–5]. These studies examined strengthening mechanisms at room temperature. More recent studies have reported the mechanical behavior of hypereutectic compositions, with even higher strength at room temperature [2,6]. Very few studies have reported the high temperature deformation behavior in Al–Sc alloys, and those dealt with hypoeutectic composition [5,6].

In this paper the creep behavior of fine-grained Al–6Mg–2Sc–1Zr alloy in the 423–533 K temperature range is presented. As Zr content in the alloy is half of Sc, Zr will replace Sc in Al_3Sc particles and Al_3(Sc, Zr) particles will form. Zirconium addition to scandium containing aluminum alloys reduces the diffusion kinetics in the alloy [1]. Threshold type creep behavior, i.e. high stress exponent and high apparent activation energy, was found from creep data analysis. Threshold stress values obtained from linear extrapolation method are compared with available theoretical models.

2. Experimental procedure

The Al–6Mg–2Sc–1Zr alloy used in present study was prepared by the powder metallurgy route. Helium atomized powder was extruded at 523 K with an extrusion ratio of 25:1. Details of the alloy design and powder processing have been reported by Kendig and Miracle [2]. Tensile tests at constant crosshead speed and creep testing at constant load

* Corresponding author. Tel.: +1-573-341-6361; fax: +1-573-341-6934.
E-mail address: rsmishra@umr.edu (R.S. Mishra).

0921-5093/$ – see front matter © 2004 Elsevier B.V. All rights reserved.
doi:10.1016/j.msea.2004.05.025

were conducted. Creep samples were prepared such that the extrusion direction corresponds to the direction of creep strain. Dog bone mini-tensile specimens were machined with 1 mm × 0.6 mm cross-section and 1.3 mm gauge length. Creep samples were machined with 2.5 mm diameter and 10 mm gauge length. Tensile creep tests were performed in air at 423, 477 and 533 K at initial strain rate ranging from 3×10^{-2} to 5×10^{-5}. Specimen elongation during creep was measured using linear voltage displacement transducer (resolution 1 μm). Some of the samples were rapidly air cooled under load after steady state was reached. This was done to retain the dislocation structure in the crept samples. Microstructural investigation of the crept samples was performed using Philips EM430 transmission electron microscope (TEM). Samples for TEM were prepared by twin jet electropolishing in 20% HNO_3 + 80% methanol solution at 240 K.

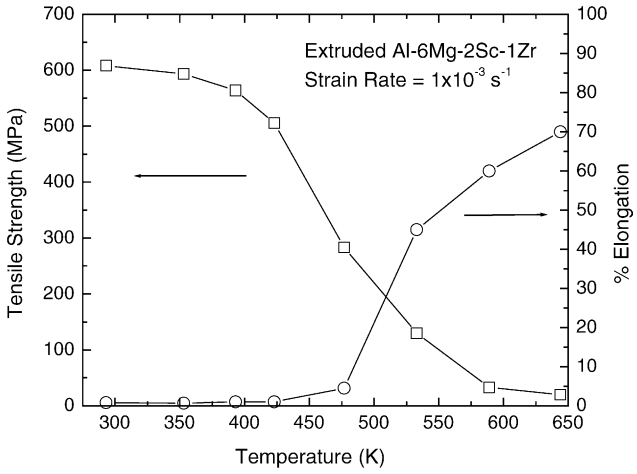

Fig. 2. Variation in tensile strength and % elongation with temperature for Al–6Mg–2Sc–1Zr alloy.

3. Results and discussion

3.1. Initial microstructure

Fig. 1a shows back-scattered electron SEM image of cross-section taken parallel to the extrusion direction. Elongation of the microstructure in the extruded direction is evident. In this image the bright spherical shape particles were identified as Al_3(Sc, Zr) using electron dispersive spectroscopy (EDS). These particles are up to 1 μm size. These relatively large primary particles are present because of large freezing range of the binary Al–Sc phase diagram [1]. The solidification rate was not sufficient to suppress the formation of these primary Al_3Sc particles through this large freezing range. The area fraction of these particles is 4.1%, as calculated from the backscattered SEM images. Fig. 1b shows the TEM bright field image of grain structure in the alloy. Mean grain size was 635 ± 105 nm (measured from 25 grains). Fine secondary Al_3(Sc, Zr), particles precipitated from the supersaturated solid solution and these can be seen in the TEM micrograph. The average size and inter-particle spacing of these particles were 7.5 and 84.4 nm, respectively. The volume fraction for the secondary Al_3(Sc, Zr) calculated from above values are 2.5%.

3.2. Tensile properties

Fig. 2 shows the change in tensile strength and % elongation with temperature at an initial strain rate of 1×10^{-3} s^{-1}. Room temperature ultimate tensile strength of the alloy was 608 MPa with 1% ductility. The strength decreases from 608 MPa at room temperature to 23 MPa at 643 K. A sharp decrease in strength can be noted above 423 K. This decrease in strengthening arises because of loss of grain boundary strengthening above this temperature. At high temperatures, dislocations can be absorbed at grain boundaries [7]. This is

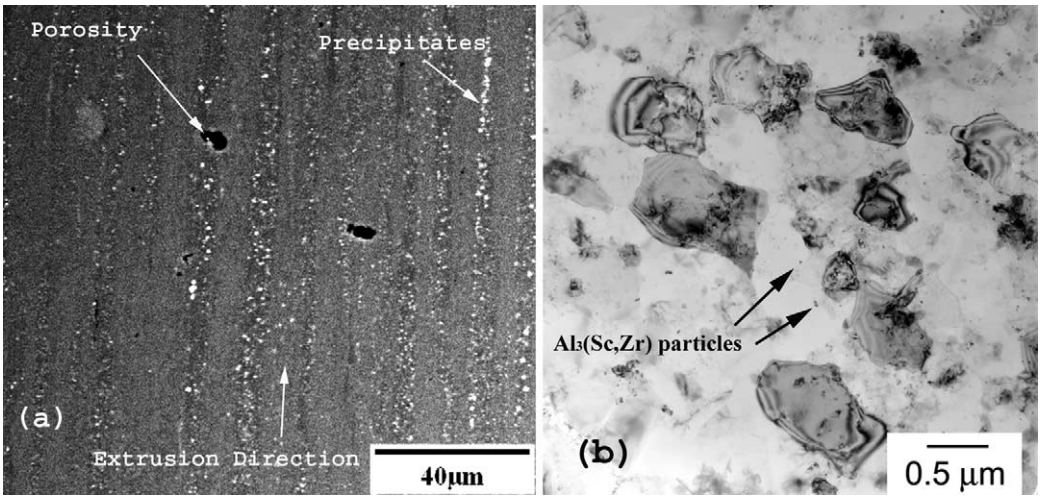

Fig. 1. (a) SEM backscattered electron image of extruded Al–6Mg–2Sc–1Zr showing primary Al_3(Sc, Zr) particles in the extruded direction. (b) Bright field TEM image of extruded Al–6Mg–2Sc–1Zr alloy showing submicron grain structure and secondary Al_3(Sc, Zr) particles.

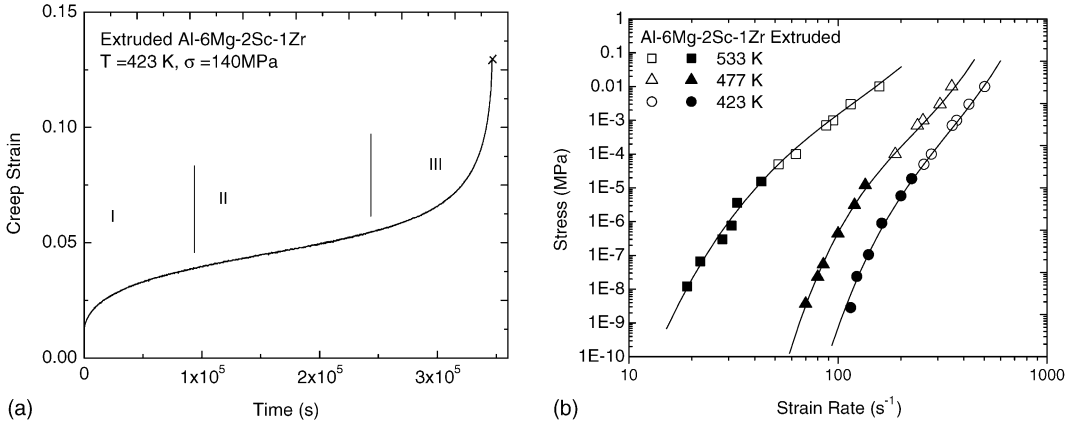

Fig. 3. (a) Typical creep curve of extruded Al–6Mg–2Sc–1Zr at 423 K and 140 MPa, and (b) plot of flow stress with minimum strain rate ($\dot{\varepsilon}_m$) for Al–6Mg–2Sc–1Zr (closed symbols indicate the creep data while the open symbols indicate data from the tensile test).

based on change in dislocation-grain boundary interaction, i.e. repulsive interaction at lower temperature to attractive interaction at elevated temperature. The increase in ductility from 4 to 45% at 473–533 K range is noteworthy.

3.3. Creep experiments

Fig. 3a shows a typical creep curve of extruded Al–6Mg–2Sc–1Zr alloy crept at 477 K and 140 MPa. Three distinct stages of creep can be identified in the curve. There is a primary stage in which the strain rate decreases with increasing time, a secondary stage where the creep rate remains reasonably constant and an extended tertiary stage where the strain rate increases with time. The magnitude and extent of creep stages, however, depend on the temperature and stress levels. Fig. 3b shows the variation of minimum strain rate with applied stress. Flow stress values at 0.1 plastic strain from the tensile data are also plotted on the same graph. These tensile tests were carried out at various initial strain rates at 423, 477 and 533 K.

A temperature compensated power law creep equation for minimum strain rate $\dot{\varepsilon}_m$ is given by [8]:

$$\dot{\varepsilon}_m = A'(\sigma)^{n_a} \exp\left(\frac{-Q_a}{RT}\right) \quad (1)$$

where A' is a constant, σ is applied stress, Q_a is apparent activation energy for creep, R is gas constant and T is absolute temperature. A modified power law creep equation for dispersion strengthened alloys is given by [8,9]:

$$\dot{\varepsilon}_m = A\frac{DGb}{kT}\left(\frac{\sigma - \sigma_0}{G}\right)^n \quad (2)$$

where A is dimensionless constant, D is lattice diffusivity, G is shear modulus, b is Burger's vector, k is Boltzmann's constant, σ_0 is threshold stress and n is true stress exponent. The apparent stress exponent n_a of minimum creep strain rate is defined as:

$$n_a = \left(\frac{\partial \ln \dot{\varepsilon}}{\partial \ln \sigma}\right)_T \quad (3)$$

This exponent increases with decreasing applied stress, which is indicative of true threshold type behavior. The threshold stress (σ_0) at various temperatures was estimated using the linear extrapolation technique [10,11]. For the value of n characterizing the operative creep mechanism the relation between $\dot{\varepsilon}_m^{1/n}$ and σ is linear at constant temperature. By extrapolation to $\dot{\varepsilon}_m = 0$ the value of σ_0 is obtained. For $n = 5$ (dislocation climb) a linear relation for the present alloy is obtained at all three temperatures (Fig. 4a). The threshold stress values estimated from this plot are 93, 57 and 6 MPa at 423, 477 and 533 K, respectively. The threshold stress decreases with increasing temperature.

An apparent activation energy (Q_a) of 181 kJ/mol was obtained using an Arrhenius plot. This value is higher than the activation energy for lattice self-diffusion of aluminum (142 kJ/mol). High n_a and Q_a is apparent values support the presence of threshold stress for creep in the alloy. After considering the effective stress ($\sigma - \sigma_0$), the present data yields an activation energy of 133 kJ/mol, which is close to 142 kJ/mol. A normalized minimum strain rates $(\dot{\varepsilon}_m kT)/(DGb)$ is plotted against normalized effective stress $(\sigma - \sigma_0)/G$ in Fig. 4b, where data for diffusivity and shear modulus of aluminum was taken form Frost and Ashby [12]. It can be seen that creep data merges are well with a regression coefficient of 0.97.

3.4. Microstructure of the crept sample

The average grain size was 275 ± 90 nm. The microstructure shows very fine coherent Al_3(Sc, Zr) precipitates of average size 8 nm. Detailed microstructural characterization of the alloy was reported earlier [2]. Fig. 5a shows a bright field TEM image of a sample crept at 477 K and 100 MPa. Interaction of multiple dislocations with a particle simultaneously can be noted. The average particle size of Al_3(Sc, Zr) mea-

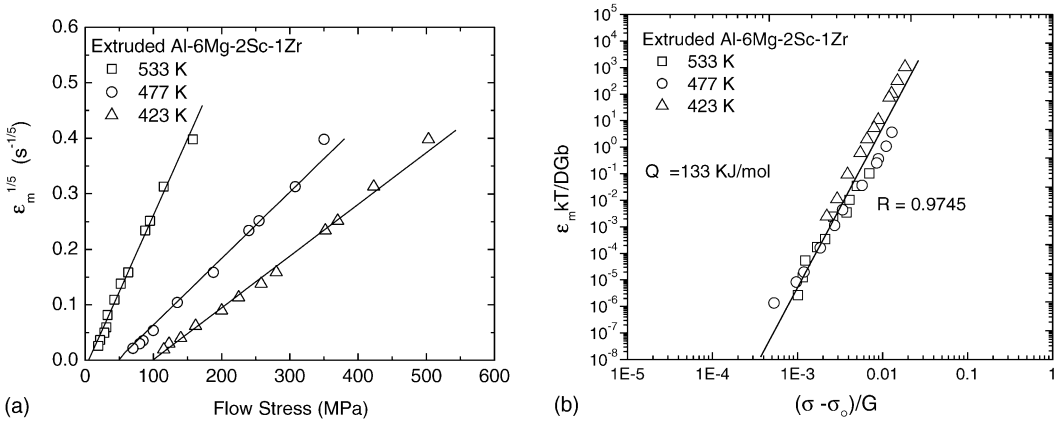

Fig. 4. (a) Plot showing estimation of threshold stress for dislocation creep, and (b) variation of temperature compensated creep rate with normalized effective stress for extruded Al–6Mg–2Sc–1Zr.

sured from the TEM images was 8.3 nm, which is similar to the particle size prior to creep (7.5 nm). This confirms that particles are thermally stable and have resistance for coarsening. Fig. 5b shows a dark field TEM image of dislocations attached on the departure side of the particles. These observations are particularly important for understanding the dislocation creep mechanism in dispersion-strengthened materials. This type of attractive dislocation-particle interaction leads to threshold stress during creep [13].

3.5. Temperature dependence of the threshold stress

Various models have been proposed for the origin of threshold stress for creep in dispersion-strengthened materials [14–17]. Fig. 6 shows a comparison of experimental threshold stresses with theoretical predictions from various models for extruded Al–6Mg–2Sc–1Zr. Orowan stress values for particle bowing which are always greater than the

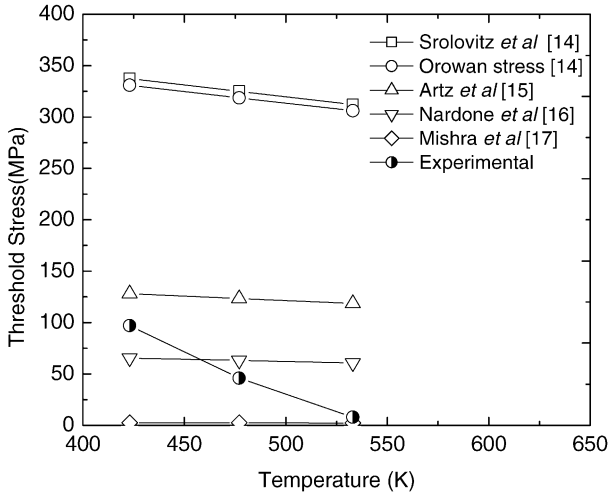

Fig. 6. Plot of threshold stress with temperature predicted by different models. Experimental values of threshold stress provided for comparison.

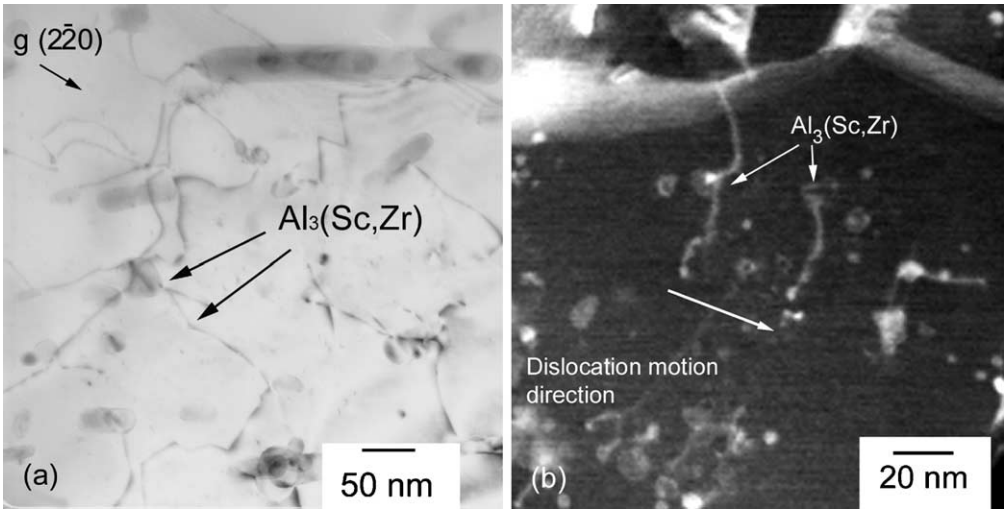

Fig. 5. (a) Bright-field TEM image showing dislocation-particle interaction, and (b) dark-field TEM image showing departure side pinning of dislocation with Al_3(Sc, Zr) particles in extruded Al–6Mg–2Sc–1Zr crept at 533 K with 120 MPa stress.

Table 1
Threshold stress values at different temperatures calculated from various models

Reference	Model	Threshold stress (MPa)		
		423 K	477 K	533 K
Orowan stress	$\frac{\sigma_0}{G} = \frac{(3.1)b}{2\pi(1-\nu)\lambda}(\ln(2) + \ln(r/r_0))$	330	318	306
Srolovitz et al. [14]	$\frac{\sigma_0}{G} = \frac{(3.1)b}{2\pi(1-\nu)\lambda}\left(\frac{\pi^2}{12} + \ln(r/r_0)\right)$	337	325	312
Artz and Wilkinson [15]	$\frac{\sigma_0}{G} = (3.1)\frac{b}{\lambda}\sqrt{1-k_A^2}$	128	123	118
Nardone et al. [16]	$\frac{\sigma_0}{E} = \left(\frac{A}{x}\right)\left(\frac{\pi r b}{2(1+\nu)\lambda}\right)$	28	27	26
Mishra et al. [17]	$\frac{\sigma_0}{G} = (3.1)A\frac{b}{\lambda}\exp\left(B\frac{r}{\lambda}\right)$	3	2	2

Material constants: $G = 26$ GPa; $b = 0.248$ nm; $\nu = 0.33$; Microstructural parameters: $\lambda = 84.4$ nm; $r = 7.5$ nm; $r_0 = b$; Model constants: (Artz) k_A =0.8 (Nardone) $A = 20$; $x = 20b$; (Mishra) $A = 0.002$; $B = 20$.

experimental observed threshold stress values, are also plotted in the same figure. The experimental threshold stress observed for the present alloy decreases with increasing temperature, which is consistent with experimental observations in other Al–Sc alloys [18,19]. Table 1 provides a summary of theoretical models used to calculate the threshold stress. None of the models are consistent with the experimentally observed temperature dependence of threshold stress. Diffusional relaxation model of Srolovitz et al. [14] predicts threshold stresses very close to Orowan stresses. Energy reduction models by Artz and Wilkinson [15] and Nardone et al. [16] predict higher values of threshold stresses at higher temperatures. The dislocation dissociation model by Mishra et al. [17] is based on the concept that dislocation energy is lowered by the dissociation of lattice dislocations at the matrix–particle interface and their transformation to interfacial dislocations. This model underestimates the threshold stress.

4. Conclusion

The Creep behavior of fine-grained Al–6Mg–2Sc–1Zr alloy was measured in a temperature range of 423–533 K. Threshold stress values of 97, 48 and 8 MPa are obtained at 423, 477 and 533 K, respectively. Microstructures of the crept samples show dislocation-particle interactions, which are responsible, for the observed threshold stress behavior in dispersion-strengthened alloys. However, none of the available theoretical models are able to account for the experimentally determined temperature dependence of the threshold stress.

Acknowledgements

The authors would like to gratefully acknowledge the support of the National Science Foundation through grant DMR-0100780. They are also thankful to Dr. Daniel Miracle of Air Force Research Laboratory for his support of this program and reviewing this paper.

References

[1] L.S. Toropova, D.G. Eskin, M.L. Kharatkterova, T.V. Dobatkina, Advanced Aluminum Alloys Containing Scandium, Gordan and Breach Science Publishers, Australia, 1998.
[2] K.L. Kendig, D.B. Miracle, Acta Mater. 50 (2002) 4165–4175.
[3] L.S. Marquis, D.N. Seidman, Acta Mater. 49 (2001) 1909–1919.
[4] R.R. Sawtell, C.L. Jensen, Metall. Trans. A 21A (1990) 421–430.
[5] E.A. Marquis, D.N. Seidman, D.C. Dunand, Acta Mater. 51 (2003) 4751–4760.
[6] R. Ünal, K.U. Kainer, Powder Metall. 41 (1998) 119–122.
[7] R.C. Pond, D.A. Smith, Philos. Mag. 36 (1977) 353–366.
[8] A.K. Mukherjee, J.E. Bird, J.E. Dorn, Trans. Am. Soc. Met. 62 (1969) 155–179.
[9] K.R. Williams, B. Wilshire, Met. Sci. J. 7 (1973) 176–179.
[10] K.T. Park, E.J. Lavernia, F.A. Mohamed, Acta Metall. Mater. 38 (1990) 2149–2159.
[11] J. Cadek, H. Oikawa, V. Sustek, Mater. Sci. Eng. A 190 (1995) 9–23.
[12] H.J. Frost, M.F. Ashby, Deformation Mechanism Maps, first ed., Pergamon Press, Oxford, UK, 1982.
[13] R.S. Mishra, A.K. Mukherjee, Light weight aluminum alloys for aerospace applications III, in: E.W. Lee, N.J. Kim, K.V. Jata, W.E. Frazier (Eds.), TMS Warrendale, PA, 1995, pp. 319–332.
[14] D. Srolovitz, R. Petkovic-Luton, M.J. Luton, Philos. Mag. 48 (1983) 795–809.
[15] E. Artz, D.S. Wilkinson, Acta Metall. 34 (1986) 1893–1898.
[16] V.C. Nardone, D.E. Matejczyk, J.K. Tien, Acta Metall. 32 (1984) 1509–1517.
[17] R.S. Mishra, T.K. Nandy, G.W. Greenwood, Philos. Mag. A 69 (1994) 1097–1109.
[18] C.B. Fuller, D.N. Seidman, D.C. Dunand, Scripta. Metall. 40 (1999) 691–696.
[19] D.N. Seidman, E.A. Marquis, D.C. Dunand, Acta Mater. 50 (2002) 4021–4035.